View metadata, citation and similar papers at core.ac.uk
brought to you by CORE
provided by Vietnam Academy of Science and Technology: Journals Online

Communications in Physics, Vol. 20, No. 1 (2010), pp. 67-75

INFLUENCE OF STRUCTURE ON OPTICAL PROPERTIES OF WO_3 THIN FILMS DEPOSITED BY SPUTTERING METHOD

LE VAN NGOC, NGUYEN DUC THINH, TRAN TUAN, DUONG AI PHUONG
University of Sciences, Vietnam National University Ho Chi Minh City
HUYNH THANH DAT
Vietnam National University Ho Chi Minh City

Abstract. *In this paper we report the synthesis of WO_3 thin films and investigate the effect of the structure on their optical properties. The WO_3 thin films are coated on glass substrates from both W and WO_3 targets by the magnetron sputtering method in ($Ar+O_2$) plasma under different deposition temperatures, varying from room temperature to 480 °C. We also evaluate the band gap energy of WO_3 by considering the transitions between the valence and the conduction bands. This result suggests that the best choices are diagonal and allowed transitions. Based on the values of band gap energy and XRD pattern, we indicate the relationship between crystalline order and optical property and consequently, the difference in color of the samples.*

I. INTRODUCTION

Tungsten oxide has been widely investigated because of their potential applications [1-2], such as in gas sensors [3-5], in catalytic, photochromic [6-7], excellent electrochromic devices [8-9] and the ability to accumulate charges [10]. However, their electrochromic properties and their optical characteristics have been focused much with hopes about some smart windows. The electrochromism is the reversible color change of thin films when they are applied under a bias and the films will be relaxed into the initial state under a reversed voltage. Therefore, their optical parameters like reflection, transmission and optical absorption can be modified by varying the external voltage or the ambient parameters. The WO_3 thin films were done by different deposition methods: spray pyrolysis [11], sol-gel [12], anodizing [13], thermal evaporation [3,14], electron beam [15] and magnetron sputtering [16-19]. Thin films, deposited by these methods, generally have a low crystallization temperature. For WO_3 films, this temperature varies from 200°C to 250°C. In case of the films, deposited by magnetron sputtering method, the growth process is highly oriented with a lot of defects. These defects not only limit the grain size, but also influence on the band gap energy E_g.

Another unique property of WO_3 thin films is the influence of crystallization order on their color. The better the films are crystallized, the more yellowish they are at the beginning stage of the electrochromic colorization. Moreover, that crystallization order also affects the color changes in the first coloration process while experimenting with the film electrochromic properties.

In this experiment procedure, WO_3 thin films are deposited by the magnetron sputtering method. The band gap energy is determined by analyzing the transmission and reflection spectra. The influences of crystallization order on the film color are explained, basing on the shift of band gap energy E_g.

II. EXPERIMENTS

Thin films WO_3 are deposited on the glass substrates by planar magnetron sputtering method with UNIVEX-450 system which can obtain the initial vacuum at 10^{-7} torr, in the gaseous mixture ($Ar + O_2$). The distance between the substrates and target is about 5 cm. We use dielectric ceramic target of WO_3, therefore the magnetron rf sputtering process is required. In this case, the heating stove is not allowed to function because of the high voltage, so the temperature of the substrate cannot be kept higher than the room temperature. In this experiment, the glass substrate is preheated to 300˚C, and during the sputtering process, it becomes cool gradually. At the ending point of sputtering process, the substrate temperature is 100˚C. However, if the metallic target W is used, the magnetron DC sputtering method could be applied and the stove will be heated continually to keep a stable temperature for a substrate during the deposition process. After being deposited, the film structure is investigated by Kristalloflex Diffraktometer (Siemens). Their thickness is measured by Stylus equipment. The transmittance and reflectance spectra are recorded by UV-2501 spectrometer. The electrochromic properties are investigated by Potentiostat.

III. DETERMINATION OF BAND GAP ENERGY

The transmittance curves in figure 1 show that WO_3 thin films absorb well ultraviolet and violet radiations. The energy of these photons is about the value of band gap energy E_g. Thus, the dependence of the absorption parameter α on the energy of incident radiation is determined by the following equation [20-21]:

$$\alpha hv = A(hv - Eg)^m \tag{1}$$

where A is a constant and E_g is the band gap energy; m has different values, depending on the type of optical transition. The possible values of m are 1/2; 3/2; 2 or 3, corresponding to various types of transitions: direct and allowed; direct and forbidden; diagonal and allowed; diagonal and forbidden, respectively. For WO_3 crystal film, the transition from the top of valence band where the state O 2p is dominant to the bottom of the conduction band which is formed by W 5d orbital is permitted.

Turning to WO_3 amorphous film, because the optical transition in the band gap is diagonal, the constant m gets the value 2 [22]. This value is used not only with amorphous films, but also with films containing grains in nano sizes [13, 22].

Figure 2 depicts the energy diagrams of crystal WO_3 monoclinic for ideal case (a) and sample with oxygen vacancies (b) [23]. In these diagrams, Γ is the point with the highest order of symmetry, corresponds to the location of ion W^{6+}. In the other words, the exchange of electrons in W-O bonds is a band transition between the top of valence band and the bottom of the conduction band. From figure 2, we realize that these points have the same coordinates in k-space in both two cases (a) and (b). Thus, the transitions,

as shown in figure 2, are direct and allowed. Furthermore, from work of Tauc et al. [20] we use the value m=1/2 for the Eq. (1).

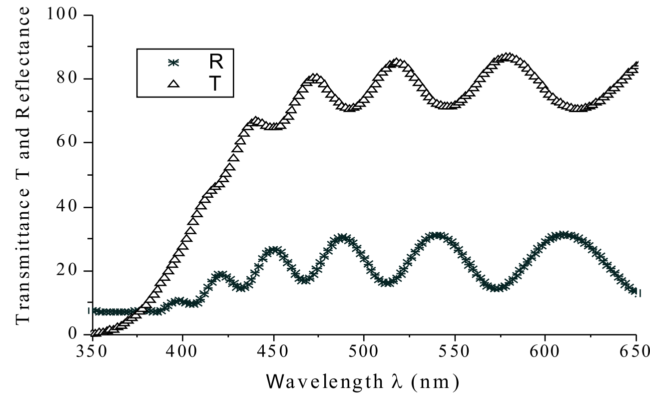

Fig. 1. The transmittance and reflectance spectra of WO_3 thin films, deposited on glass substrates at 480˚C by magnetron DC sputtering method with W target.

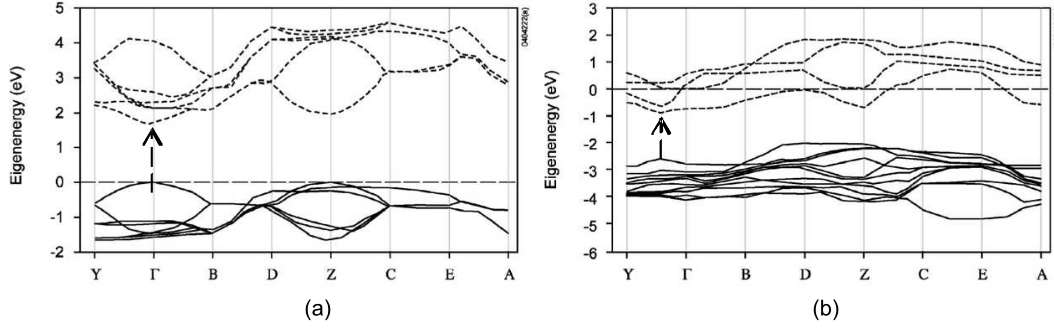

Fig. 2. The energy diagram of crystal WO_3 – monoclinic for the ideal sample (a) and sample with oxygen vacancies (b) [23].

In these thin films WO_3, there are always some defects and the sizes of the crystals WO_3 are determined in the range 20-40 nm by Scherrer formula. One of the problems in calculating the band gap energy E_g by the formula (1) is that we can not know exactly which the type of optical transitions is, because our films are not totally amorphous ($m = 2$) either crystallized ($m = 1/2$). These films are a mixture of small crystalline particles in the amorphous ambience and some oxygen vacancies. Thus, based on the equation (2) and experimental data, we determine the value of band gap energy E_g for both the two values of m:

$$(\alpha h\upsilon)^{1/m} = A(h\upsilon - Eg) \tag{2}$$

with A is a constant; the absorption coefficient α is a function of wavelength λ [24]:

$$\alpha_{(\lambda)} = \frac{1}{d}\ln\left(\frac{1 - R_{(\lambda)}}{T_{(\lambda)}}\right) \tag{3}$$

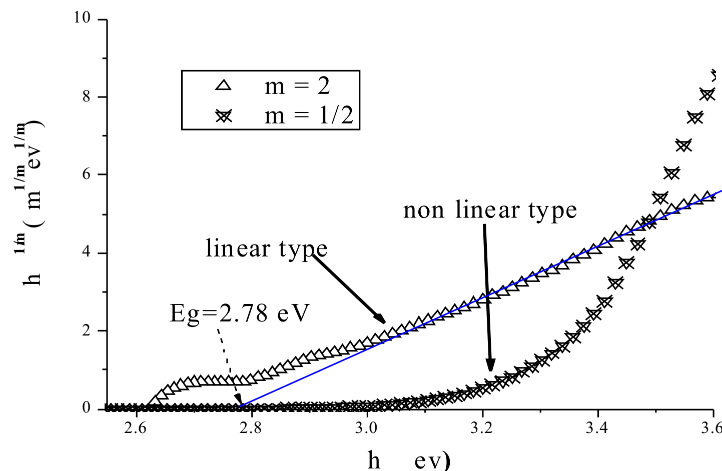

Fig. 3. The dependence of $(\alpha h\nu)^{1/m}$ on absorbed photon energy $h\nu$ with the two values of m (m=2 and m=1/2). For m=1/2, the unit in the vertical axis is 10^2.

$T_{(\lambda)}$ and $R_{(\lambda)}$ are the transmission and reflection indexes, respectively and are measured directly by the equipment UV-2501 (see Fig. 1). All the films are well crystallized with the average grain size around 37 nm.

Figure 3 shows the dependence of $(\alpha h\nu)^{1/m}$ upon the absorbed energy $h\nu$ for two cases with m=2 and m=1/2. From that figure, it is considered that when m=2 our function is well linear in the interval from 2.6eV to 3.6eV (E_g = 2.78eV), whereas for m=1/2 the function is nonlinear, but exponential. The same calculations for all our films, their pairs of graphs for m=2 and m=1/2 have the same forms as shown in figure 3: a linear line for m=2 and an exponential curve for m=1/2. It means that the value m=2 is more suitable. This assumption is supported by the fact that the linearity of the graph for the case m=2 and E_g are almost unchanged after multiplying by $d^{1/2}$ as shown in figure 4b. Therefore, we choose m=2 to determine the band gap energy E_g.

IV. INFLUENCES OF CRYSTALLIZATION STATE ON THE BAND GAP ENERGY

Table 1. Band gap energy of thin films WO_3, deposited by RF method with WO_3 target.

P_{total} (torr)	Substrate temperature = RT		Substrate temperature = 300°C →100°C	
	Thickness (nm)	E_g (eV)	Thickness (nm)	E_g (eV)
1×10^{-3}	750	3.28	750	3.15
3×10^{-3}	540	3.35	440	3.26
5×10^{-3}	300	3.39	400	3.27

Table 1 describes the calculating results of E_g for films, deposited by magnetron rf method. These results reveal the fact that the higher the pressure of working gas is, the

larger the band gap is. Moreover, a band gap energy of film which is deposited at room temperature is larger than ones of films, deposited at higher temperature.

The changing of E_g can be interpreted basing on cluster – type structure model. It is suggested that the amorphous films consist of clusters in which there are 3 or more WO_6 octahedral. These clusters with sizes between 1 and 10 nm [2] are disposed randomly. When the deposition temperature exceeds the crystallization point (staying on 200 – 250 $^{\circ}$C for WO_3 film, deposited by magnetron sputtering), there is a phase transition in the films, some clusters grow and form single crystals in which the clusters are arrayed orderly. Therefore, the film crystallization at the beginning is a function of time – coating and the kinetic energy of reaching substrate – particles. Moreover, both the small clusters at a few nanometers, corresponding with an amorphous phase and tiny single crystal are the causes that make the band gap values larger than the band gap value of bulk material. Thus, the band gap energy will rise with the decrease of the average clusters' size or the decrease of substrate temperature.

Several experimental SEM results show that the average of the clusters' size depends on substrate's temperature and coating particles' kinetic energy. In films deposited by thermal evaporation method, this kinetic energy is rather small $\sim$ 0.1 eV [25], so that with the unheated substrates, the clusters' size is about 1nm [26] and about 3 nm for 150°C substrates [27]. Turning to magnetron sputtered method, in which the coating particle has a higher kinetic energy (ranging from 1 to 40 eV [25]), these values are 2 – 8 nm [28] and 10 nm [29], corresponding to unheated and 185 $^{\circ}$C substrates. After all, increasing the substrates' temperature (under crystallization point) and coating particles' kinetic energy, the clusters' size will be grown.

The values of E_g deposited by rf magnetron sputtering on Table 1 indicate that when increasing total working pressure, the band gap energies become larger. In case of films, deposited onto substrate at room temperature, these values are 3.28 eV and 3.39 eV if the total working pressures are 1 mtorr and 5 mtorr, respectively. For the films, coated on a preheated substrates (starting at 300 $^{\circ}$C and ending at 100 $^{\circ}$C), when the temperature is above the crystallization point, a crystalline phase is formed in WO_3 films and when the temperature is below this point, only the amorphous phases are formed. Thus the band gap values are relative small, ranging from 3.15 eV to 3.27 eV, corresponding to 1 mtorr and 5 mtorr.

To investigate band gap energy of WO_3 with high crystallization, films are deposited by magnetron DC sputtering method from metallic target W with stable substrate temperature. Deposition parameters and values of band gap energy are listed in Table 2. The crystallization state and the determination of the band gap energy are presented in figure 4.

Figure 4(a) depicts XRD patterns which inform well about the crystalline structure of WO_3films with different crystallization states, reported in the same conditions. Samples noted by a, b, c and d, show a good crystallization with the (001) peak only (2θ are between 22° and 22.5°). The inset is XRD patterns of samples e, f in the small angle regions. The crystallization in sample e is quite bad and sample f gives out only a small peak which is

Table 2. Band gap energy E_g of WO_3 films, deposited by magnetron DC method.

Samples	$I_{sputter}$ (A)	T (°C)	t (minute)	d (nm)	E_g (eV)
a	0.2	300	20	1950	2.67
b	0.15	300	20	1030	2.76
c	0.2	480	10	710	2.78
d	0. 15	480	10	500	2.80
e	0.15	250	10	470	3.03
f	0.15	200	10	410	3.14

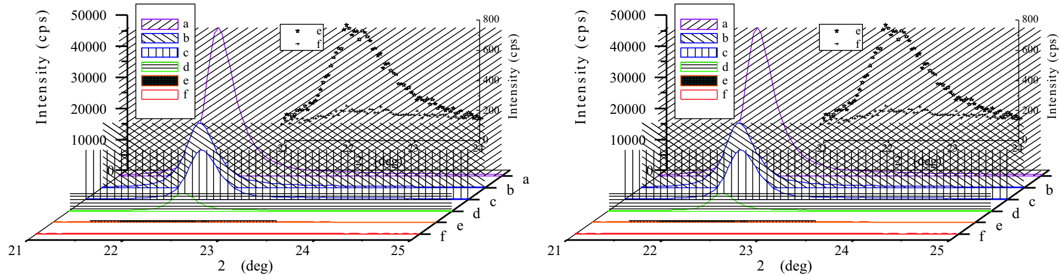

Fig. 4. The influences of crystalline structure on band gap energy. (a) XRD patterns of crystalline structures of thin films, the inset in the top right for e, f sample; (b) Plot of $(\alpha dh\nu)^{1/2}$ versus $h\nu$ to determine E_g.

only a signal of crystallization. Fig. 4(b) is a linear graph which shows the dependence of $(\alpha dh\nu)^{1/2}_{(h\nu)}$ upon E_g, listed in Table 2.

Figure 4 reveals that the film, which gets the higher XRD peak intensity, gives the smaller band gap value. In the other words, the longer the path which the light penetrates through crystalline phases is, the smaller E_g is. Our data is also well consistent with the results of Takaya Kubo and Yoshinori Nishikitani [30] in which the ratio between the amount of double bonds W=O (at the boundaries of grains) and the single bonds O-W-O (inside the octahedral) increases (the crystallization is worsening) with the raise of E_g.

V. INFLUENCES OF CRYSTALLIZATION ORDER ON ABSORPTION EDGE AND COLOR OF THIN FILMS

The above results also elucidate about the relationships between crystallization order and the red shift of absorption edge (Fig. 5). It's because of a strong absorption in violet region when light penetrates through our samples. Thus, after exiting, the light gets a small shift to yellow color and the well-crystallized films are always yellowish.

When films are colored by the electrochromic process, electrons and ion H^+ (or Na^+, Li^+, K^+) are injected into films, and form small polarons in films. Larg Berggren's experiments [21]and V.V.Bryksin's theory [31] indicate that these polarons absorb the radiation in the red and infrared regions very well. Consequently, the transmission spectra have a low intensity in the long wavelength region. The rise of potential in the electrochromic

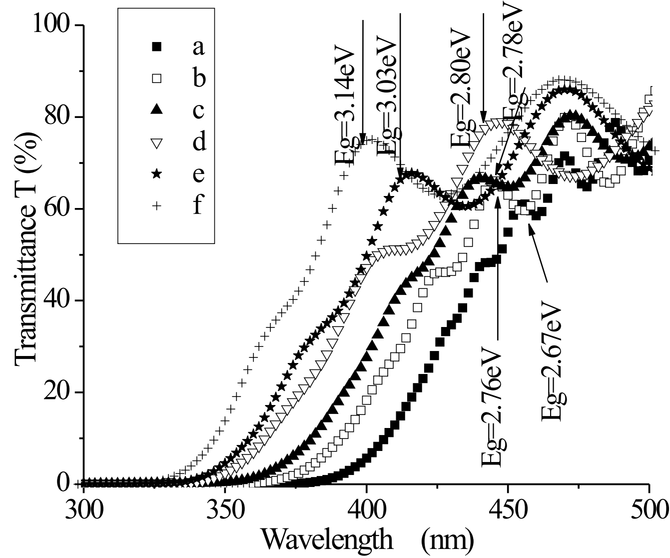

Fig. 5. The shift to the longer wavelength of the absorption edge of WO_3 films with the decrease of the band gap energy.

process will raise the density of polarons in films, and make the red and infrared radiation to be absorbed more. This will result in the gradual shift of their color coordination to the blue region. So, for the well crystallized films, whose color coordination is at first located in the yellow region, in the coloring process, this color coordination will move to the colorless region, and then step by step to the blue and dark blue regions, as shown in the figure 6. In the bleaching process, the bias is reversed, the electrons and ions are ejected from films, the color coordination returns back, but it usually stops at the colorless region. Therefore, in the next coloring process, films show green and then blue color earlier than it does in the first process. In the case of the amorphous films or low-ordered films, they are often colorless and turns to green color more quickly than the well-crystallized films do.

VI. CONCLUSIONS

From the experimental results, we can conclude that the grain size of WO_3 thin films, deposited by magnetron sputtering method stays in 20 – 40 nm gap, the optical transitions of these films are diagonal and allowed and the absorption obeys the equation $(\alpha h\upsilon)^{1/2} = A(h\upsilon - Eg)$.

Moreover, the band gap energy of films depends on the values of the total working pressure and the substrate temperature. With the sputtering process works in higher pressure (ranging from 1 mtorr to 5 mtorr), the band gap of film is wider. By the way,

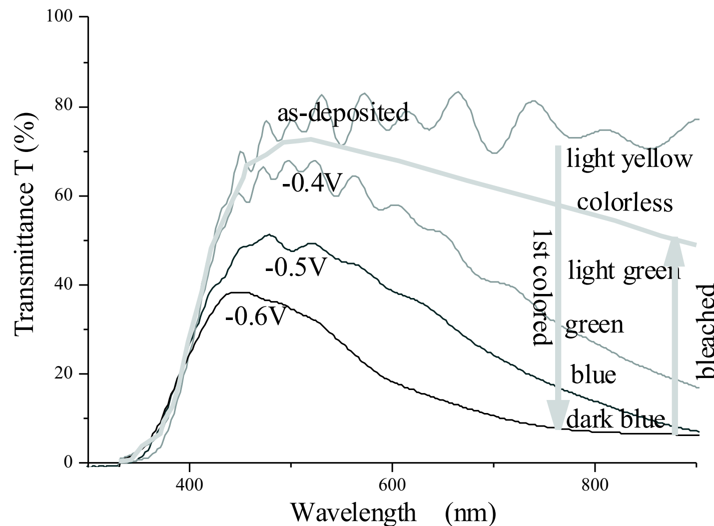

Fig. 6. The transmittance spectra of WO_3 thin films, colored in the solution HCl 1M under the bias: -0,4V; -0,5V and -0,6V. The right side arrows indicate the color change.

film is deposited on the higher temperature substrate (ranging from the room temperature to the crystallization point) will gives the band gap more narrow.

Finally, there exists the relationship between the crystallization order of films and the red shift of the absorption edges in the transmission spectra. This seems to be the reason of the yellow color of the films in the beginning stage of colorization process. For films with better crystallization, it appears the green color requiring the longer passing path of the color coordination.

REFERENCES

[1] K. Bange, *Solar Energy Materials & Solar Cells* **58** (1999) 1-131.
[2] C. G. Granqvist, *Handbook Inorganic Electrochromic Materials*, Elsevier, Amsterdam, 1995.
[3] Nguyen Thi Bao Ngoc, Nguyen Van Nha, Nguyen Van Minh, *Proc. 2nd IWOMS* 1995, pp. 341-344.
[4] Nguyen Van Nha, Nguyen Thi Bao Ngoc, Nguyen Van Hung, *Thin Solid Film* **334** (1998) 113.
[5] K.H. Lee, Y.K. Fang, W.J. Lee, J.J. Ho, K.H. Chen, K.S. Liao, *Sens. Actuators* **B69** (2000) 96.
[6] S.K. Deb, *Solar Energy Materials & Solar Cells* **92** (2008) 245–258.
[7] Pham Duy Long, M.C. Bernard, Nguyen Thi Tu Oanh, A.Hugot-Le Goff, and Nguyen Nang Dinh. *Proc. IWOS'2000*, pp. 473-476.
[8] Vu Thi Bich, Nguyen Thanh Binh, Nguyen Thi Bich Ngoc, and A.Hugot-Le Goff, *Proc. IWOS'2000*, pp. 477-480.
[9] C.G. Granqvist, E. Avendano and A. Azens, *Thin Solid Film* **442** (2003) 201.
[10] Karl-Heinz Heckner, Alexander Kraft, *Solid state Ionics* **152-153** (2002) 899-905.
[11] M. Regragui, M. Addou, A. Outzourhit, Elb. El Idrissi, A. Kachouane, and A. Bougrine, *Solar Energy Materials & Solar Cells*, **77** (2003) 341-350.
[12] Toshikazu Nishide, Fujio Mizukami, *Thin Solid Films* **295** (1995) 212-217.

[13] M.J. Hutchins, N.A. Kamel, N. El-Kadry, A.A. Ramadan, K. Abdel-Hady, Phys. Stat. Sol. (a) **175** (1999) 991.
[14] P.V. Ashrit, Thin Solid Films **385** (2001) 81-88.
[15] P. D. Long, N. V. Hung, N. N. Dinh, N. D. Thao, *Proc. 2nd IWOMS* 1995, pp. 267-270.
[16] Thi. M. Pham, G. Velasco, and Revue Chim, *Minerale* **22** (1986).
[17] Huiyao Wang, Pei Xu, Tianmin Wang, *Thin Solid Films* **388** (2001) 68-72.
[18] Le Van Ngoc, Tran Tuan, Nguyen Van Den, Duong Ai Phuong, Huynh Thanh Dat, Tran Cao Vinh, and Cao Thi My Dung, *Science & Technology Development VNU-HCMC*, **8** (1) (2005) 29-33.
[19] Le Van Ngoc, Le Quang Tri, Tran Tuan, Huynh Thanh Dat, Duong Ai Phuong, and Nguyen Van Den, *Science & Technology Development VNU-HCMC*, **11** (06) (2008) 67-72.
[20] J. Tauc, R. Grigoro Vici and A. Vancu, *Phys. Stat. Sol.* 15 (1966) 627-637.
[21] Lars Berggren, Ph.D thesis, Acta Universitatis Upsaliensis, Uppsala, Swedden, (2004), 49.
[22] C.G. Granqvist, Solar Energy Materials & Solar Cells **60** (2000) 201-262.
[23] R. Chatten, A.V. Chadwick, A. Rougier, P.J.D. Lindan, *J. Phys. Chem.* **B109** (2005) 3146.
[24] F. Abeles, *Progress in Optics*, **2** (1963) 249-251.
[25] H. K. Pulker, Coatings on glass, *Thin films Science and Technology*, *Elsevier* **6** (1984), 246.
[26] C. Kaito, T. Shimizu, Y. Nakata and Y. Saito, *Japan. J. Appl. Phys.* 24 (1985) 117-120.
[27] M. Shiojiri, T. Miyano, and C. Kaito, *Japan. J. Appl. Phys.* **18** (1979) 1937-1945.
[28] T. Nanba and I. Yasui, *J. Solid State Chem.* **83** (1989) 304-315.
[29] D. Green and A. Travlos, *Philos. Mag.* **B51** (1985) 521-532.
[30] Takaya Kubo and Yoshinori Nishikitani, *J. Electrochem. Soc.* **145** (5) (1998) 1729-1734. (The Electrochemical Society, Inc.)
[31] V. V. Bryksin, *Sov. Phys. Solid State*, **24** (1982) 627 – 631.

Received 05 May 2009.